NASA TECHNICAL MEMORANDUM

NASA TM X-834

(NASA TM X-834)

PRESSURE DISTRIBUTION ON A BLUNT-LEADING-EDGE MODIFIED-DELTA-PLANFORM REENTRY CONFIGURATION AT A MACH NUMBER OF 6.0

by J. Wayne Keyes
Langley Research Center,
Langley Station, Hampton, Va.

NATIONAL AERONAUTICS AND SPACE ADMINISTRATION • WASHINGTON, D. C. • SEPTEMBER 1963

TECHNICAL MEMORANDUM X-834

PRESSURE DISTRIBUTION ON A BLUNT-LEADING-EDGE MODIFIED-DELTA-PLANFORM REENTRY CONFIGURATION AT A MACH NUMBER OF 6.0

By J. Wayne Keyes

Langley Research Center
Langley Station, Hampton, Va.

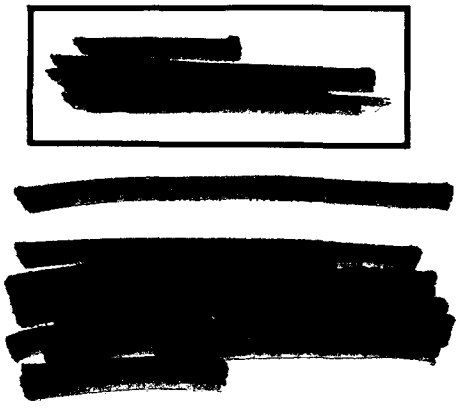

NATIONAL AERONAUTICS AND SPACE ADMINISTRATION

NATIONAL AERONAUTICS AND SPACE ADMINISTRATION

TECHNICAL MEMORANDUM X-834

PRESSURE DISTRIBUTION ON A BLUNT-LEADING-EDGE MODIFIED-DELTA-PLANFORM REENTRY CONFIGURATION AT A MACH NUMBER OF 6.0*

By J. Wayne Keyes

SUMMARY

An investigation was conducted at a Mach number of 6.0 to determine the pressure distribution on a blunt-leading-edge modified-delta-planform body at angles of attack from 44.4° to 89.0° and a Reynolds number of 2.3×10^6 (based on the maximum chord of the delta planform).

A comparison of the experimental pressure data with values obtained by using modified Newtonian theory indicates that the theory generally predicts the trend and the relative magnitude of the local pressures. The main areas of disagreement are on the rounded edges where the pressures are generally overpredicted and on the bottom flat surface where the pressures are underpredicted when a stagnation pressure region occurs at a lower angle of attack than that predicted by theory. A hypersonic five-term series approximation and a method based on sweep angle and Mach number give a good prediction of the measured pressures near the centroid of the bottom flat surface; an expression based on sweep theory and impact theory gives a good prediction of the pressure variation normal to the leading edge of the delta planform. The values of body normal-force and axial-force coefficients obtained from the integration of the theoretical pressure distribution predict the general trend of the measured force coefficients.

INTRODUCTION

The use of aerodynamic lift during reentry into the earth's atmosphere has been under investigation for some time. Some previous studies (refs. 1 to 6) have found that the use of lift during reentry results in a greater range of allowable reentry angles for a given peak deceleration and allows a wider choice of landing sites. Two drawbacks to the use of lift are the increase in vehicle weight for a given payload requirement and the resulting increase in heat input (ref. 2).

---

*[redacted]

As part of a general research program, several reentry configurations with a maximum hypersonic lift-drag ratio of about 1/2 and a wide variation in shape have been investigated; a summary of the force data is presented in reference 7. The pressure distribution on one of these configurations, a blunt-leading-edge modified-delta-planform body (designated L-3), is given in the present paper. Pressure distributions on other configurations as well as delta wings are presented in references 8 to 11.

The purpose of this investigation is to compare the measured pressure distribution on the L-3 configuration with that predicted by modified Newtonian theory and other methods. Modified Newtonian predictions are also compared with measured force data. The L-3 configuration was tested over an angle-of-attack range from 44.4° to 89.0° at a Mach number of 6.0, a Reynolds number of 2.3×10^6 (based on the maximum chord of the delta planform), a stagnation pressure of 26 atmospheres, and a stagnation temperature of 500° F.

SYMBOLS

A,B,D	constants
C_A	body axial-force coefficient, $\frac{F_A}{q_\infty S}$
C_N	body normal-force coefficient, $\frac{F_N}{q_\infty S}$
C_p	pressure coefficient, $\frac{p_l - p_\infty}{q_\infty}$
$C_{p,min} = -\frac{1}{M_\infty^2}$	
F_A	axial force, lb
F_N	normal force, lb
M_∞	free-stream Mach number
p_l	local static pressure, lb/sq in. abs
p_∞	free-stream static pressure, lb/sq in. abs
q_∞	free-stream dynamic pressure, lb/sq in. abs
r	delta-planform leading-edge radius, in.

R	radius of cylindrical portion of model afterbody, in.
s	surface distance, in.
s'	modified surface distance normal to leading edge of delta planform, in. (see ref. 10)
S	projected area of delta planform, sq in.
X,Y,Z	body axes
x,y,z	coordinates of pressure-orifice location, in. (see fig. 2 and table I)
α	angle of attack, measured relative to bottom flat surface, deg
η	angle between velocity vector and vector normal to body surface, deg

$$\xi = \frac{C_p - C_{p,min}}{C_{p,max} - C_{p,min}}$$ (see ref. 10)

Subscript:

max	stagnation condition behind normal shock wave

APPARATUS AND MODEL

Tunnel

This investigation was conducted in the Langley 20-inch Mach 6 tunnel which is an intermittent type exhausting into the atmosphere. It can operate at a maximum stagnation pressure of about 37 atmospheres and a stagnation temperature of 600° F. A more complete description of the tunnel is given in reference 12.

Model

The model is composed of a blunt-leading-edge modified delta planform with an afterbody that is essentially shielded from the flow at high angles of attack, as stated in reference 7. The leading-edge radius decreases with increasing distance from the nose. A drawing and photograph of the model are shown in figure 1(a) and figure 1(b), respectively. All dimensions are based on a value of R of 2.00 inches, which is the radius of the cylindrical portion of the model afterbody.

The model was instrumented with 55 pressure orifices located on one-half of the model since it was symmetrical with respect to the XZ-plane. Figure 2 is a schematic drawing of the model with orifice locations indicated along 12 rays.

The coordinates of each orifice with respect to the body-axis system shown in figure 2 are presented in table I.

Support System

The model was mounted on a support system which rotates in the vertical plane to provide an angle-of-attack range from 0° to 90°. The support system can be translated vertically to keep the model located near the center of the tunnel. A photograph of the support system is shown as figure 3 of reference 8.

MEASUREMENTS AND ACCURACY

The pressure orifices were connected to several valves that sequentially sample the pressures. Two transducers, one with a range of 0 to 5 lb/sq in. abs and one with a range of 0 to 15 lb/sq in. abs, were attached to each valve in order to obtain more accurate data. Each transducer was accurate to 0.5 percent of full scale. The accuracy of C_p was within ± 0.012. Angle-of-attack measurements are accurate to within $\pm 0.2^{\circ}$.

Previous tunnel calibrations have shown that the tunnel Mach number may vary from 5.94 to 6.04 as a function of test time and 0.02 throughout the test section at a given time. Therefore, in order to reduce the data, the maximum local pressure measured on the model for each angle of attack was used to compute the Mach numbers. This calculation was made by assuming a normal shock loss in the stagnation region and by using the ratio of the maximum local pressure to the tunnel stagnation pressure. The Mach number calculated was always within the calibrated range from 5.94 to 6.04.

RESULTS AND DISCUSSION

Typical schlieren photographs of the model at various angles of attack are shown in figure 3. Analysis of the schlieren photographs indicates flow separation on the forward flat surface at $\alpha = 44.4^{\circ}$; however, the separation appears to have occurred behind the most rearward pressure orifice and there is no discernible increase in pressure.

The pressure distribution along rays I to XII is presented in figures 4 to 9. The pressure coefficient C_p is plotted as a function of a nondimensionalized surface distance ratio. For comparative purposes, the local leading-edge radius was used to nondimensionalize the surface distances for rays III to VI in figure 6 because of the leading-edge-radius variation. Modified Newtonian theory defined as

$$C_p = C_{p,max} \cos^2 \eta$$

where $C_{p,max} = 1.818$ for a Mach number of 6.0, was used to predict the pressure distribution on all rays. In general, modified Newtonian theory predicted the trend of the data but did not give a good approximation of the local measured pressure distribution.

As expected, modified Newtonian theory did not predict the three-dimensional-flow effects on the bottom flat surface as seen in figures 4, 6, 7, and 8(a). In a manner similar to that reported in references 8 and 11, the theory underpredicts the local pressures on the bottom surface except near an angle of attack of 90° and overpredicts the pressures near the bottom surface edge with the deviation increasing as angle of attack increases. Therefore, there is a strong pressure relieving effect near the edges of the bottom flat surface. As also noted in references 8 and 11, a stagnation region was measured on the bottom flat surface at an angle of attack of about 65° although modified Newtonian theory predicts it only at 90°. However, the theory gives a good prediction of the pressure distribution on the nose at angles of attack where a stagnation pressure was measured. (See fig. 4.) The reason for this agreement can be explained by an examination of the schlierens (fig. 3) where the bow shock is seen to be close to the surface of the nose at the moderate angles of attack.

A comparison of the pressures measured on the leading edge of the delta planform with those predicted by theory is presented in figures 6 and 8 and indicates that, in general, the measured pressures for a given value of s/r decrease with increasing distance from the nose above $\alpha = 58.8°$. The variation as stated previously is caused by the relieving effects along the swept leading edge and trailing edge. The measured pressures remain fairly constant with station on the aft surfaces in the higher α range as observed in figures 6 and 9.

In figure 10, the pressures on the center line of the bottom flat surface predicted by several methods are compared with measured pressure data. A hypersonic five-term series approximation of the pressure coefficient (curve A) was obtained from reference 10. Curves B and C were calculated by a method derived in reference 13. Free-stream Mach numbers of 6 and ∞ were used in the calculations of the data for curves B and C, respectively. The Newtonian prediction for a flat plate is given by curve D. If the pressure measured near the centroid of area of the bottom flat surface is used to minimize edge effects, good agreement is obtained with curve A except at the lower angles of attack. In general, curves A and B bracket the measured data over the entire angle-of-attack range.

A comparison of the pressures measured normal to the leading edge of the delta planform with those obtained by an expression related to sweep and impact theory (ref. 10) is presented in figure 11. The ordinate scale is defined by

$$\xi = \frac{C_p - C_{p,min}}{C_{p,max} - C_{p,min}}$$

and the abscissa scale $\frac{s'}{r}$ is defined with $\frac{s'}{r} = 0$ at the point of tangency of the flow direction and the leeward leading-edge surface. The expressions $A \sin^2 \frac{s'}{r}$, $B \sin^2 \frac{s'}{r}$, and $D \sin^2 \frac{s'}{r}$ were obtained in the same manner as in

reference 10, and the values of A, B, and D were obtained from curves A, B, and D, respectively, in figure 10 for given angles of attack. When $\frac{s'}{r} = 1.57$ radians, maximum pressure is supposedly realized on the delta planform surface and the expressions reduce to the values of ξ indicated by the constants A, B, and D. The expression $A \sin^2 \frac{s'}{r}$ predicts the trend of the pressure variation and, in general, the values on the curved surfaces near the nose of the delta planform.

Since the theoretical pressure distribution has been calculated for a complicated body such as the L-3, it is of interest to see how well the integrated theoretical pressure distributions agree with the measured force coefficients reported in reference 7, which have been corrected for base pressure effects. Figure 12 shows that the integrated curves generally predict the trend of the measured normal- and axial-force coefficients. At the moderate angles of attack up to about 65° on the C_N curve and 82° on the C_A curve, theory underpredicts the force coefficients. This variation can be primarily attributed to the underestimation of pressures on the bottom flat surface in the case of C_N. Above 65° angle of attack the measured values of C_N are overpredicted since there are extreme pressure relieving effects around the edges of the bottom surface.

CONCLUSIONS

An investigation was made at a Mach number of 6 to determine the pressure distributions on a blunt-leading-edge modified-delta-planform configuration at angles of attack from 44.4° to 89.0° and a Reynolds number of 2.3×10^6 based on the maximum chord of the delta planform. A comparison of measured data with theoretical data indicated the following conclusions:

1. Modified Newtonian theory generally predicts the trend and the relative magnitude of the pressure distribution. The main areas of disagreement are on the bottom flat surface, except in the higher angle-of-attack range, where the average pressures are underpredicted, and near and on the rounded edges where the pressures are generally overpredicted.

2. Stagnation pressure occurs on the bottom flat surface at a lower angle of attack than that predicted by modified Newtonian theory.

3. A hypersonic five-term series approximation and a method based on sweep angle and Mach number give a good prediction of the measured pressures near the centroid of area of the bottom flat surface.

4. An expression based on sweep theory and impact theory gives a good prediction of the pressure variation normal to the leading edge of the delta planform.

5. The values of body normal-force and axial-force coefficients obtained from the integrated theoretical pressure distribution predict the general trend of the measured force coefficients.

Langley Research Center,
National Aeronautics and Space Administration,
Langley Station, Hampton, Va., April 25, 1963.

REFERENCES

1. Lees, Lester, Hartwig, Frederic W., and Cohen, Clarence B.: Use of Aerodynamic Lift During Entry Into the Earth's Atmosphere. ARS Jour., vol. 29, no. 9, Sept. 1959, pp. 633-641.

2. Becker, John V.: Re-Entry From Space. Scientific American, vol. 204, no. 1, Jan. 1961, pp. 49-57.

3. Chapman, Dean R.: An Analysis of the Corridor and Guidance Requirements for Supercircular Entry Into Planetary Atmospheres. NASA TR R-55, 1960.

4. Eggers, Alfred J., Jr., and Wong, Thomas J.: Re-Entry and Recovery of Near-Earth Satellites, With Particular Attention to a Manned Vehicle. NASA MEMO 10-2-58A, 1958.

5. Becker, J. V., Baradell, D. L., and Pritchard, E. B.: Aerodynamics of Trajectory Control for Re-Entry at Escape Speed. Astronautica Acta, Vol. VII, Fasc. 5-6, 1961, pp. 334-358.

6. Grant, Frederick C.: Importance of the Variation of Drag With Lift in Minimization of Satellite Entry Acceleration. NASA TN D-120, 1959.

7. Rainey, Robert W., compiler: Summary of Aerodynamic Characteristics of Low-Lift-Drag-Ratio Reentry Vehicles From Subsonic to Hypersonic Speeds. NASA TM X-588, 1961.

8. Holloway, Paul F.: Pressure Distribution on a Flat-Bottom Canted-Nose Half-Cone Reentry Configuration at a Mach Number of 6.0. NASA TM X-736, 1962.

9. Staylor, W. Frank, Sterrett, James R., and Goldberg, Theodore J.: Pressure Distributions on a Blunt-Nose Lifting Reentry Body With Flaps at a Mach Number of 6.0 With Emphasis on the Nature of the Local Flow. NASA TM X-766, 1963.

10. Mueller, James N. (With appendix by Eugene S. Love): Pressure Distributions on Blunt Delta Wings at a Mach Number of 2.91 and Angles of Attack up to 90°. NASA TM X-623, 1962.

11. Goldberg, Theodore J., and Hondros, James G.: Pressure Distributions on a Flat-Plate Delta Wing Swept 65° at a Mach Number of 5.97 at Angles of Attack From 65° to 115° and Angles of Roll From 0° to 25° at a 90° Angle of Attack. NASA TM X-702, 1962.

12. Sterrett, James R., and Emery, James C.: Extension of Boundary-Layer-Separation Criteria to a Mach Number of 6.5 by Utilizing Flat Plates With Forward-Facing Steps. NASA TN D-618, 1960.

13. Fetterman, David E.: A Method for Predicting the Normal-Force Characteristics of Delta Wings at Angles of Attack From 0° to 90°. NASA TM X-757, 1963.

TABLE I.- COORDINATES OF PRESSURE ORIFICES

Ray	s/R	x, in.	y, in.	z, in.
I	1.26	1.37	0.00	-0.79
	1.89	2.12	.00	.21
	1.99	2.22	.00	.38
	2.11	2.27	.00	.61
	2.22	2.22	.00	.84
	2.34	2.09	.00	1.03
	2.45	1.91	.00	1.15
	2.57	1.66	.00	1.20
	2.75	1.32	.00	1.20
	2.92	.96	.00	1.20
	3.27	.26	.00	1.20
	3.62	-.43	.00	1.20
	3.73	-.65	.00	1.20
	4.07	-1.34	.00	1.20
	4.22	-1.62	.00	1.08
	4.38	-1.74	.00	.80
	4.68	-1.74	.00	.16
	5.18	-1.74	.00	-.79
II	0.00	1.66	0.00	1.20
	.13	1.87	-.12	1.15
	.25	2.05	-.21	1.01
	.38	2.15	-.28	.79
	.49	2.17	-.30	.56
Ray	s/r	x, in.	y, in.	z, in.
III	0.00	1.66	0.00	1.20
	.42	1.79	-.18	1.16
	.84	1.89	-.36	1.01
	1.30	1.94	-.45	.79
	1.68	1.94	-.46	.58
	2.00	1.94	-.44	.40
	2.35	1.92	-.42	.21
IV	-0.86	0.96	0.00	1.20
	.00	1.18	-.35	1.20
	.43	1.30	-.53	1.15
	.90	1.38	-.68	1.01
	1.33	1.44	-.76	.82
	1.73	1.44	-.78	.63
	2.59	1.41	-.72	.21
V	-1.95	0.26	0.00	1.20
	.00	.71	-.71	1.20
	1.73	.94	-1.09	.67
	2.82	.90	-1.04	.20
VI	-3.79	-0.65	0.00	1.20
	-2.48	-.41	-.39	1.20
	.00	.07	-1.20	1.20
	.86	.21	-1.44	1.03
	1.73	.26	-1.51	.74

Ray	s/R	x, in.	y, in.	z, in.
VII	0.00	0.43	0.00	1.20
	.20	-.41	-.39	1.20
	.74	-.40	-1.48	1.20
	.91	-.40	-1.72	1.05
	1.03	-.40	-1.81	.80
VIII	0.00	0.26	0.00	1.20
	.40	-.41	-.39	1.20
	.81	-1.11	-.82	1.20
	.96	-1.35	-.97	1.08
	1.12	-1.45	-1.02	.80
IX	0.00	1.66	0.00	1.20
	.30	1.18	-.35	1.20
	.60	.71	-.71	1.20
	1.00	.07	-1.20	1.20
	1.28	-.40	-1.48	1.20
	1.75	-1.11	-.82	1.20
	2.18	-1.34	.00	1.20
X	0.00	2.09	0.00	1.03
	.12	2.05	-.21	1.01
	.23	1.89	-.36	1.01
	.53	1.38	-.68	1.01
	1.23	.21	-1.44	1.03
	1.58	-.40	-1.72	1.05
	1.72	-.67	-1.64	1.05
	2.18	-1.35	-.97	1.08
	2.67	-1.62	.00	1.08
XI	0.00	2.27	0.00	0.61
	.16	2.17	-.30	.56
	.30	1.97	-.46	.58
	.70	1.44	-.78	.63
	.90	.94	-1.09	.67
	1.30	.26	-1.51	.74
	1.67	-.40	-1.81	.80
	1.84	-.74	-1.73	.80
	2.36	-1.45	-1.02	.80
	2.90	-1.74	.00	.80
XII	0.00	2.12	0.00	0.21
	.10	2.12	-.20	.21
	.26	1.92	-.42	.21
	.56	.90	-1.04	.20
	.87	1.41	-.72	.21
	1.48	-.14	-1.66	.21
	1.59	-.35	-1.72	.21
	1.74	-.65	-1.72	.21
	2.83	-1.74	.00	.16

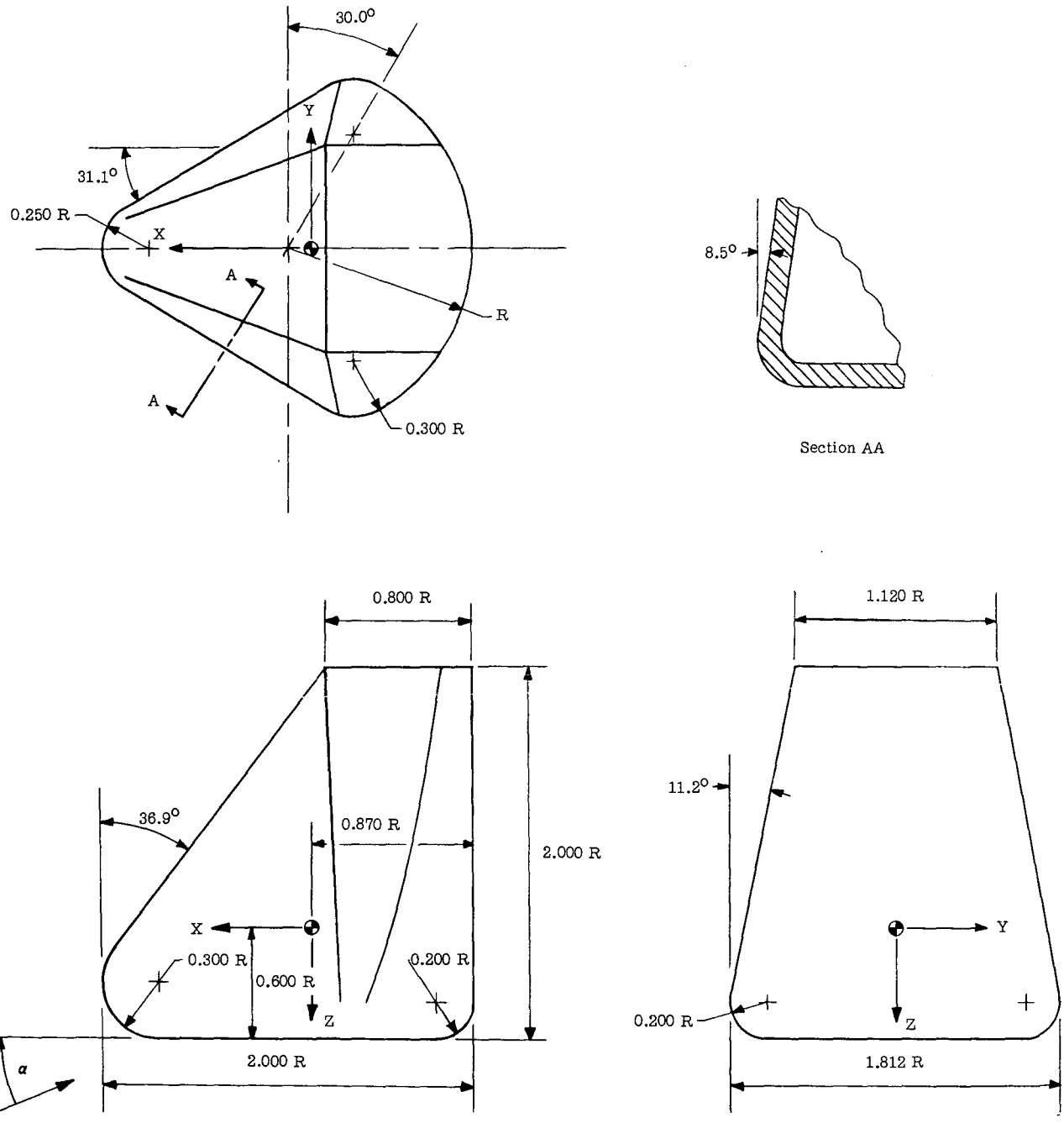

(a) Drawing of model showing dimensions. R = 2.000 in.

Figure 1.- Model of L-3 configuration used in the investigation.

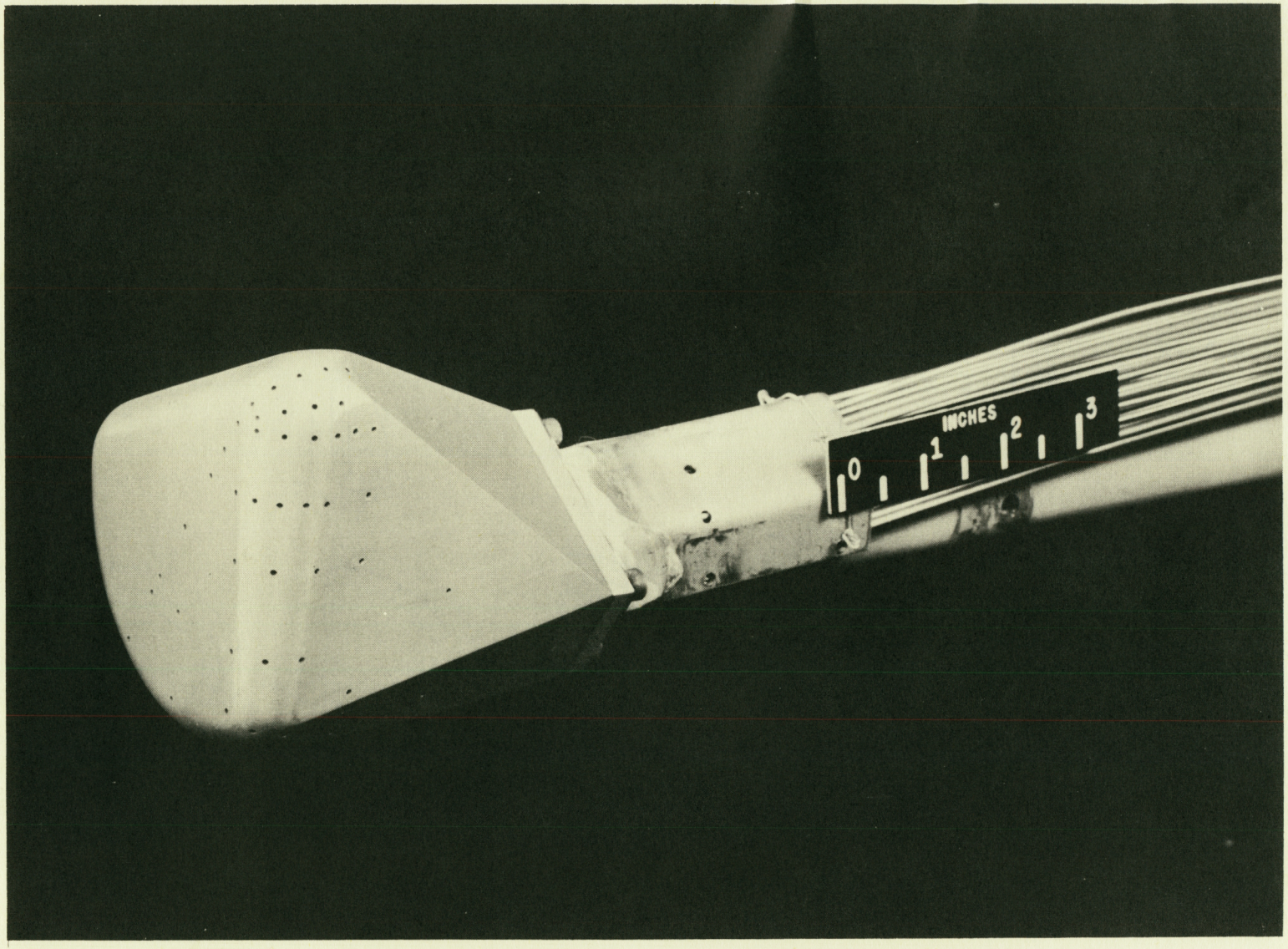

(b) Model mounted on support. L-61-644

Figure 1.- Concluded.

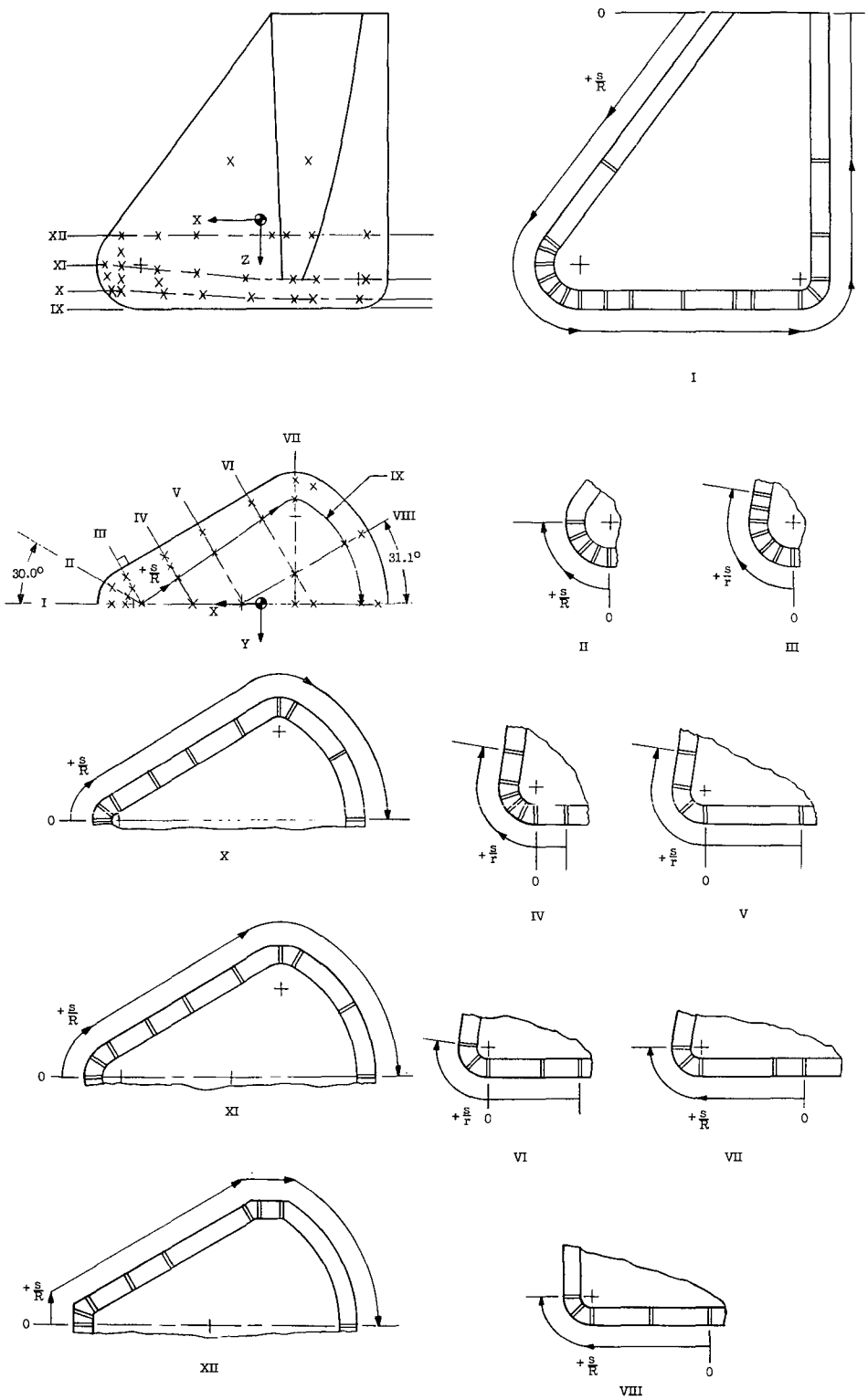

Figure 2.- Sketch showing location of pressure orifices.

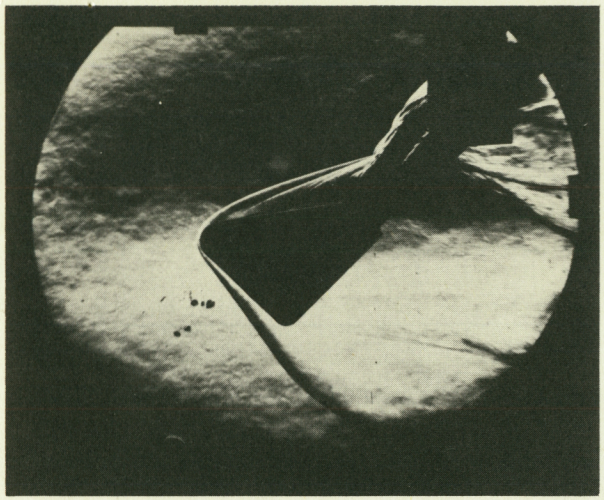

$\alpha = 44.4^\circ$

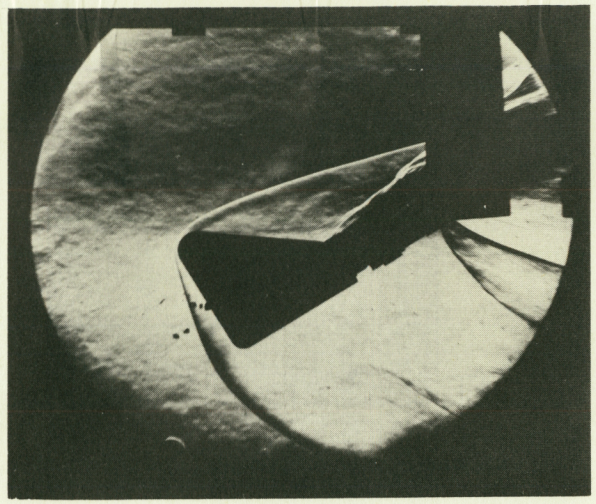

$\alpha = 58.8^\circ$

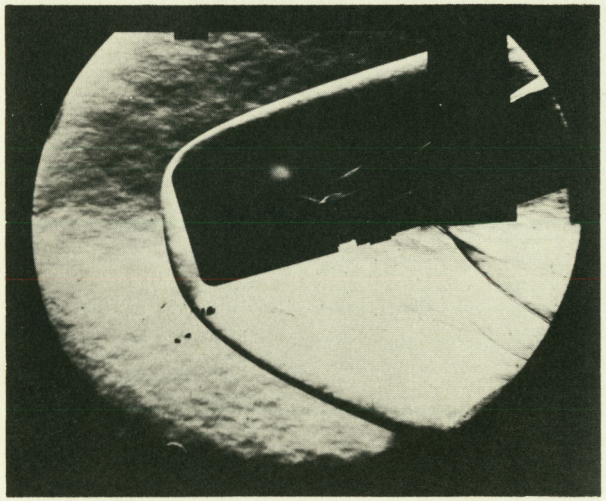

$\alpha = 74.1^\circ$

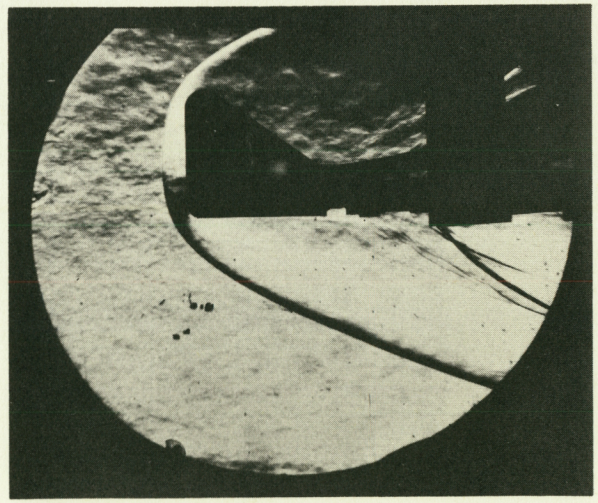

$\alpha = 89.0^\circ$

Figure 3.- Schlieren photographs of the model at various angles of attack. L-63-3150

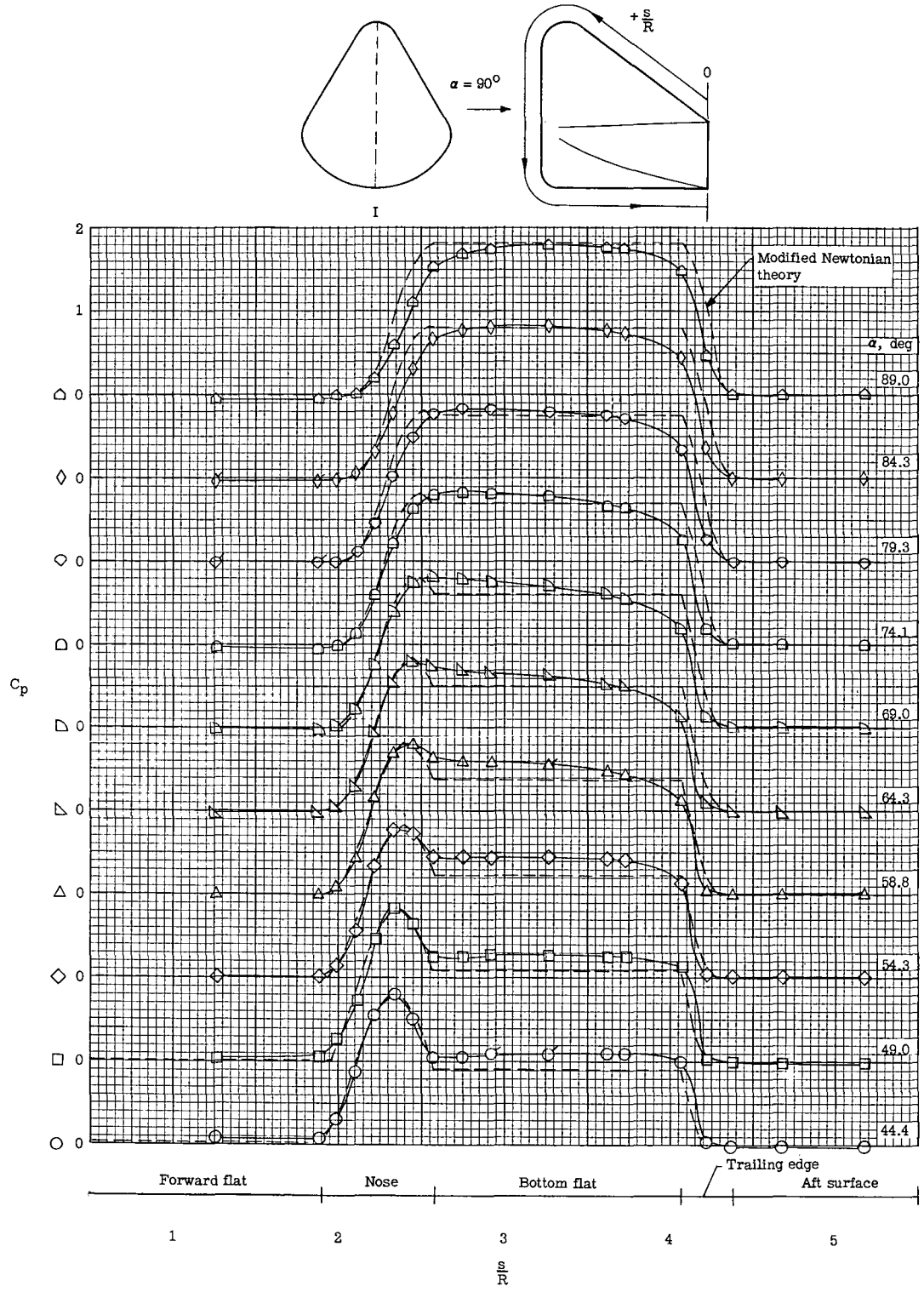

Figure 4.- Pressure distribution along ray I. (Flagged symbols indicate interpolated data.)

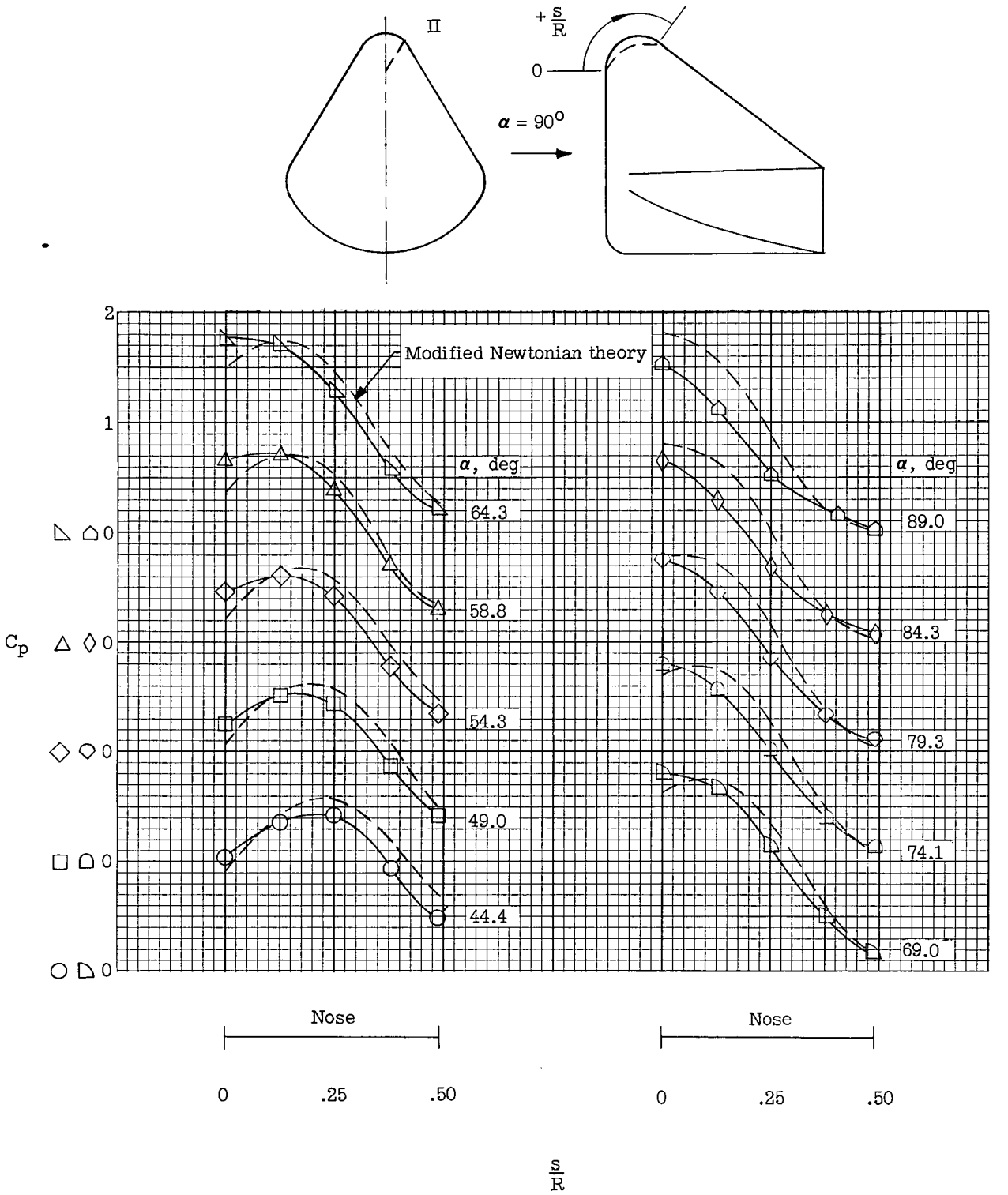

Figure 5.- Pressure distribution along ray II. (Flagged symbols indicate interpolated data.)

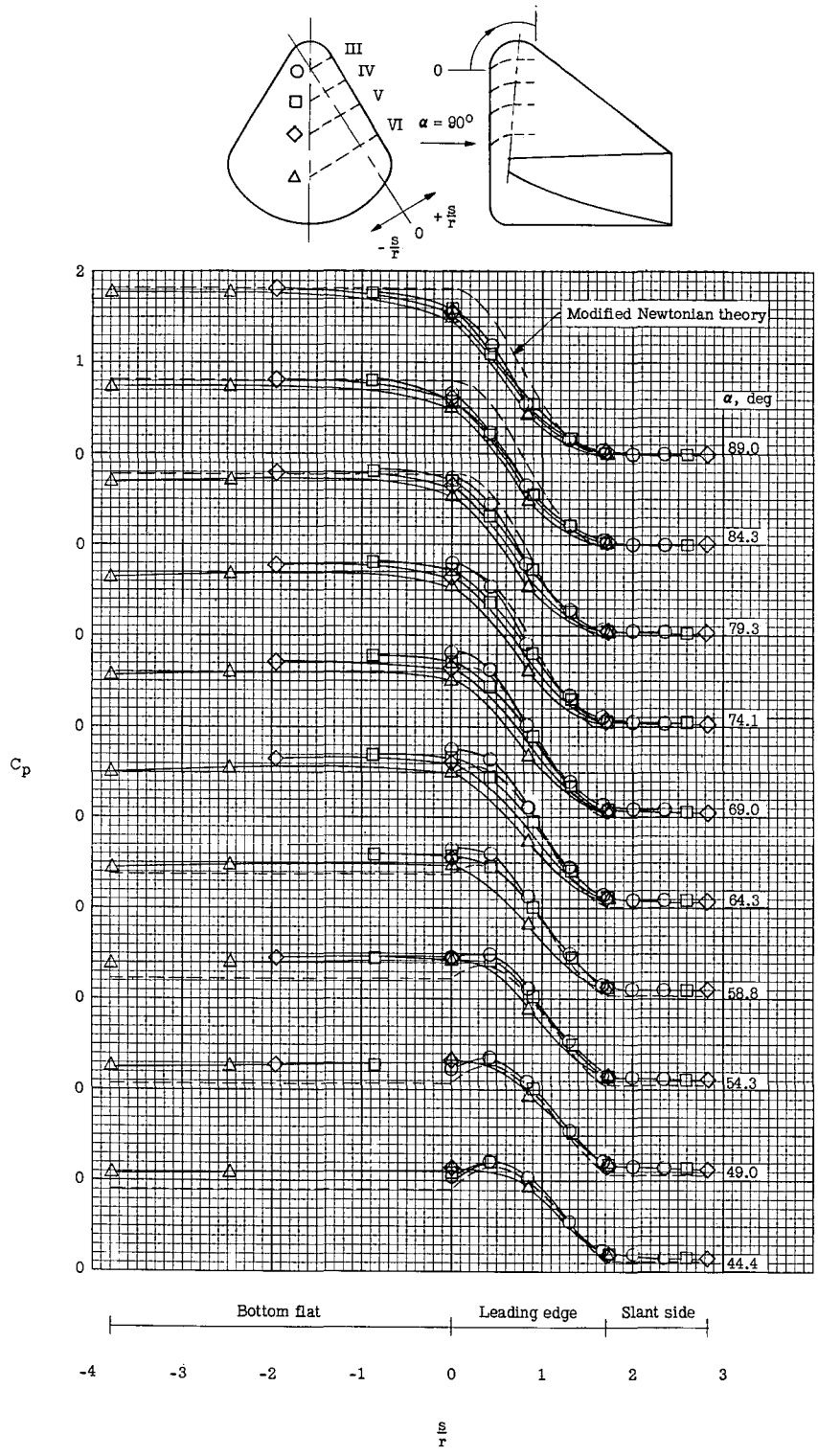

Figure 6.- Pressure on leading edge of delta planform (ray III to ray VI).

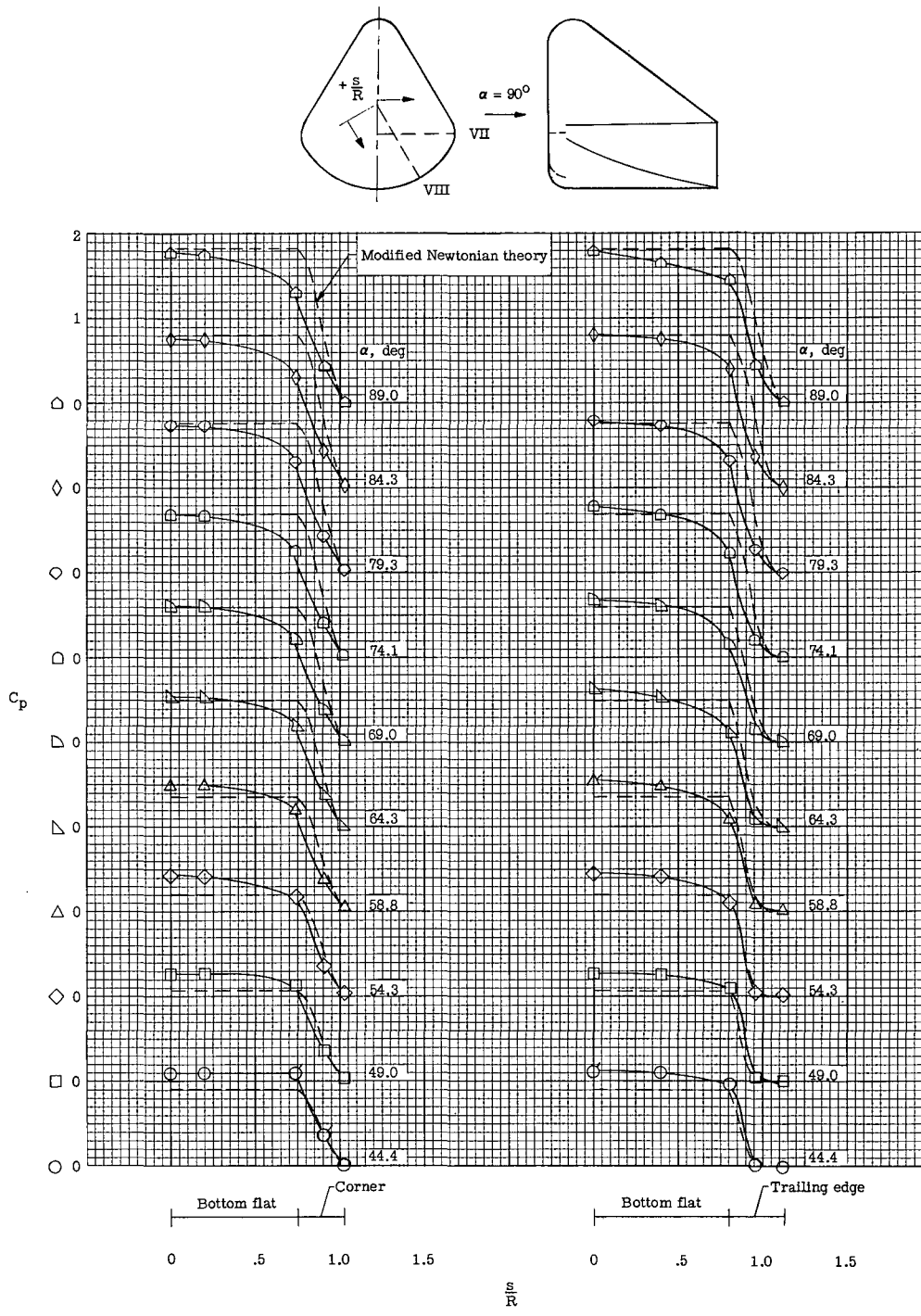

(a) Ray VII. (b) Ray VIII.

Figure 7.- Pressure distribution along ray VII and ray VIII. (Flagged symbols indicate interpolated data.)

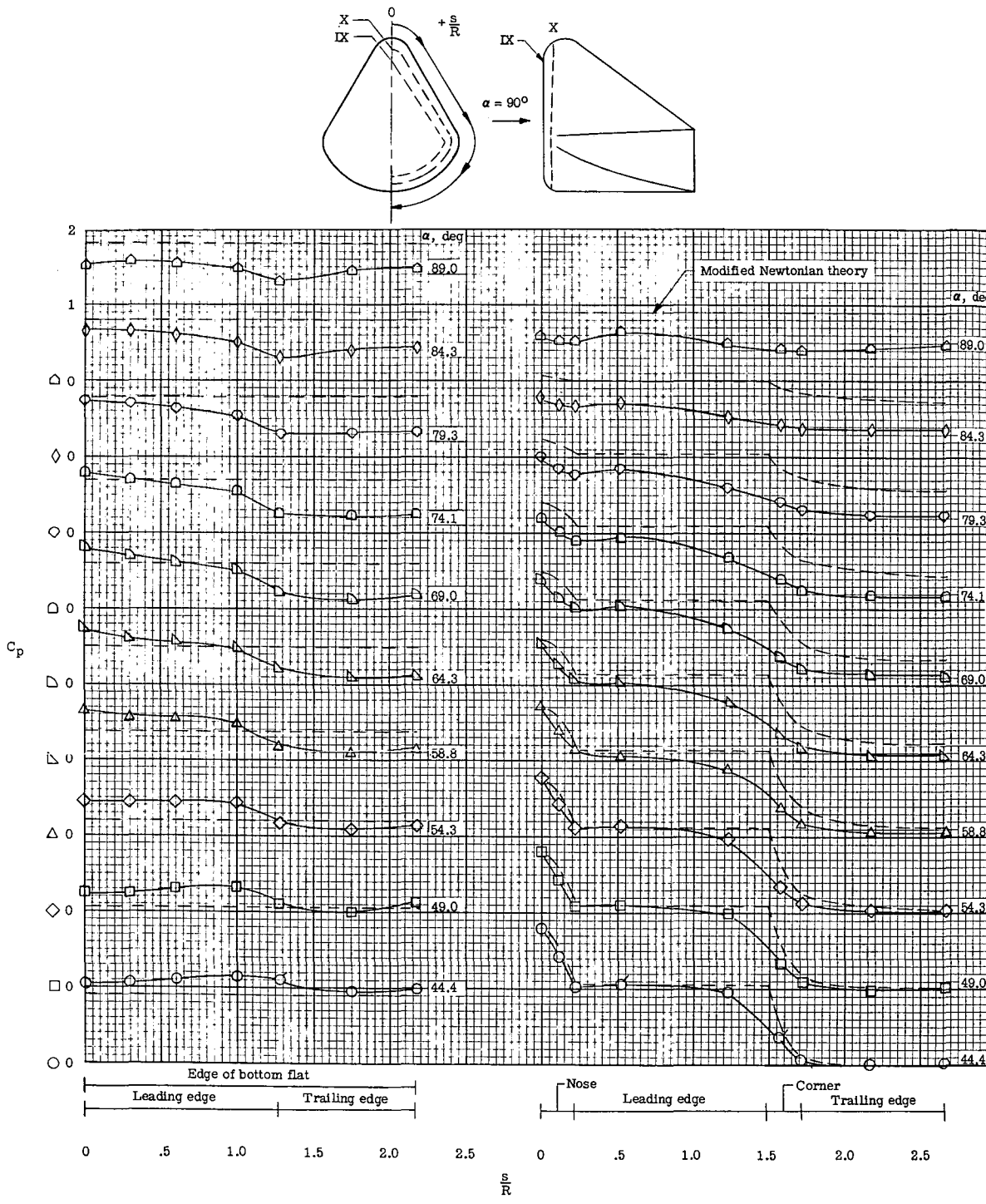

(a) Ray IX (s/r = 0).

(b) Ray X (s/r = 0.785).

Figure 8.- Pressure distribution along ray IX and ray X. (Flagged symbols indicate interpolated data.)

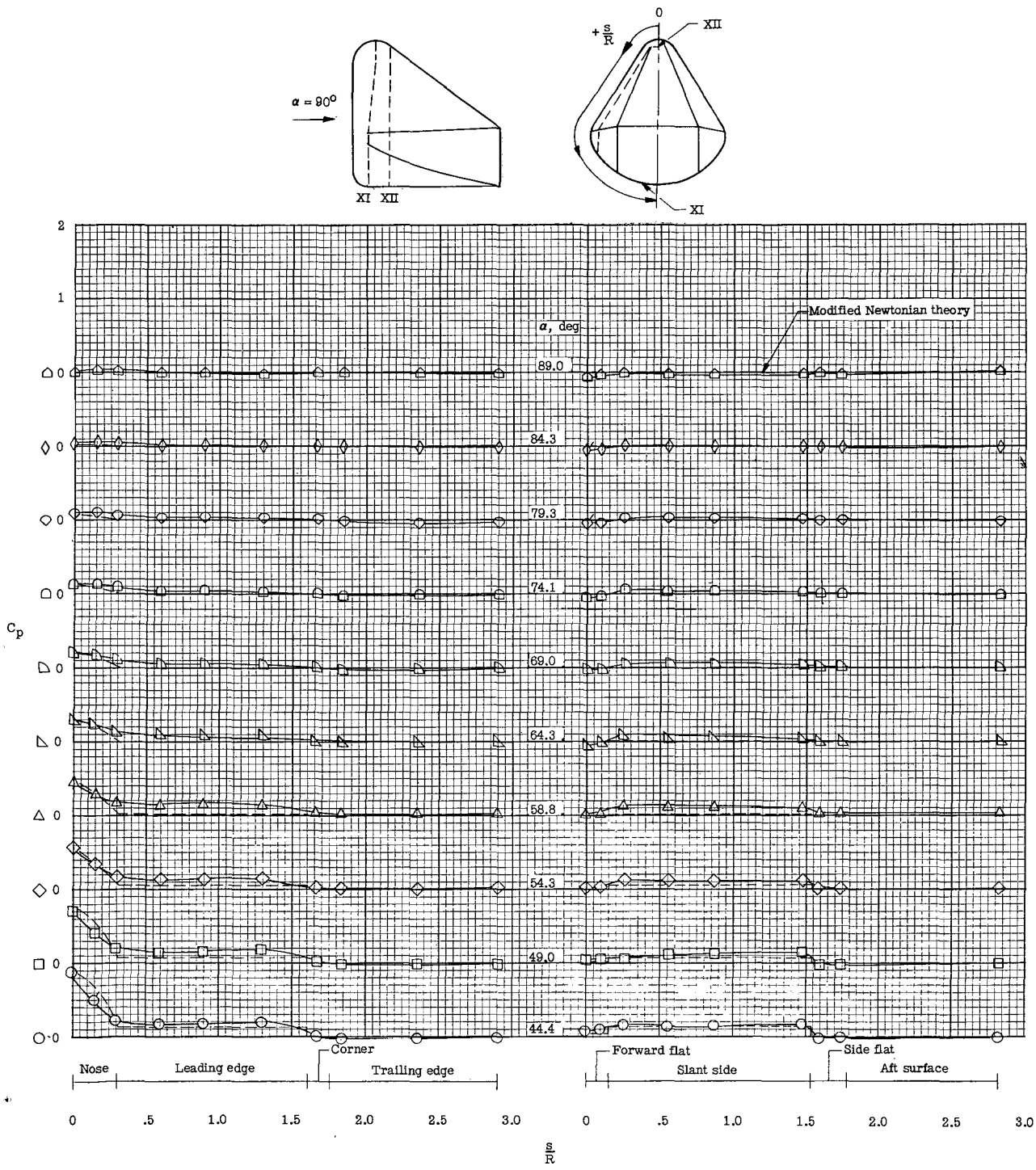

(a) Ray XI (s/r = 1.571). (b) Ray XII.

Figure 9.- Pressure distribution along ray XI and ray XII. (Flagged symbols indicate interpolated data.)

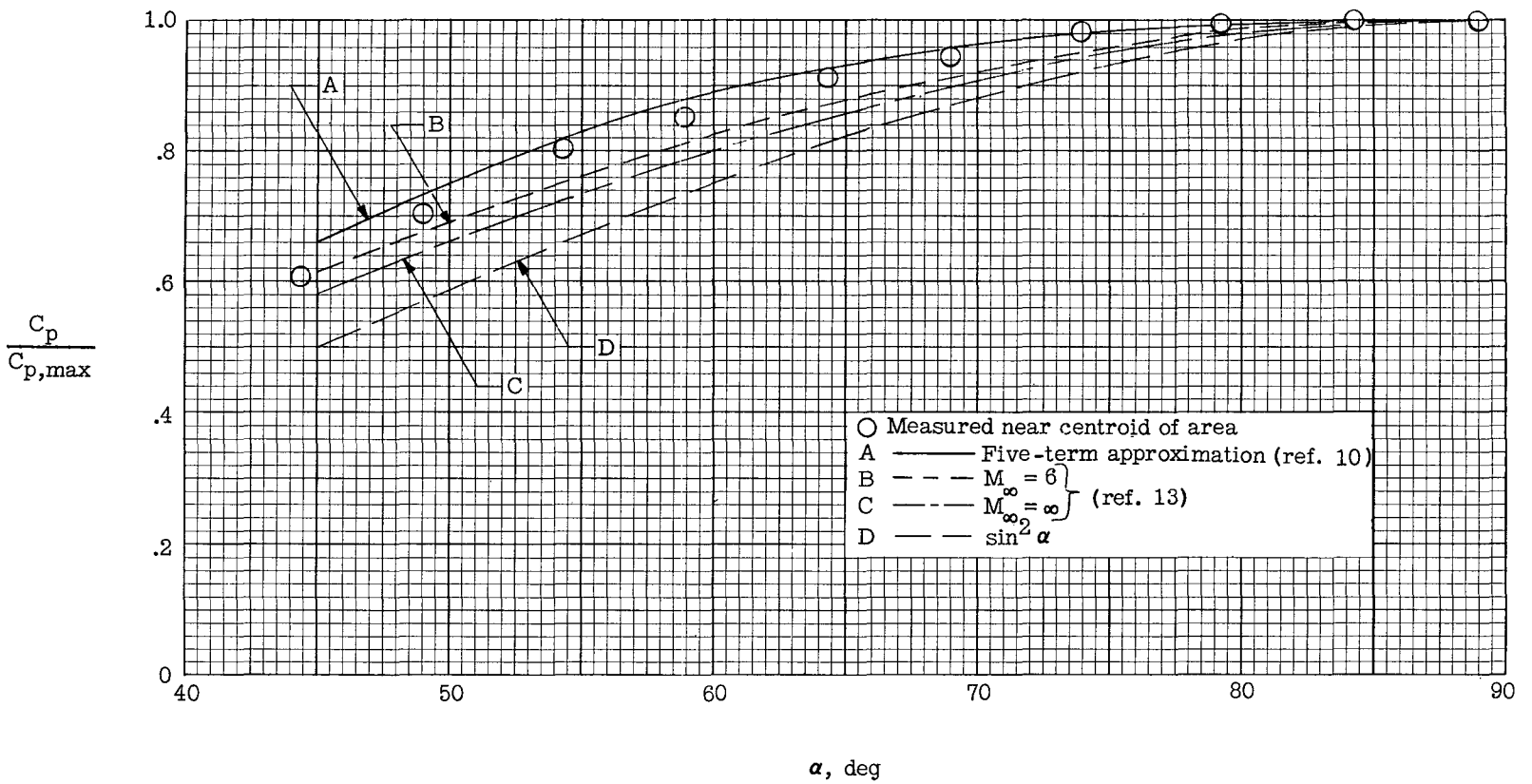

Figure 10.- Comparison of measured pressure data on bottom flat surface with data obtained by several theoretical methods.

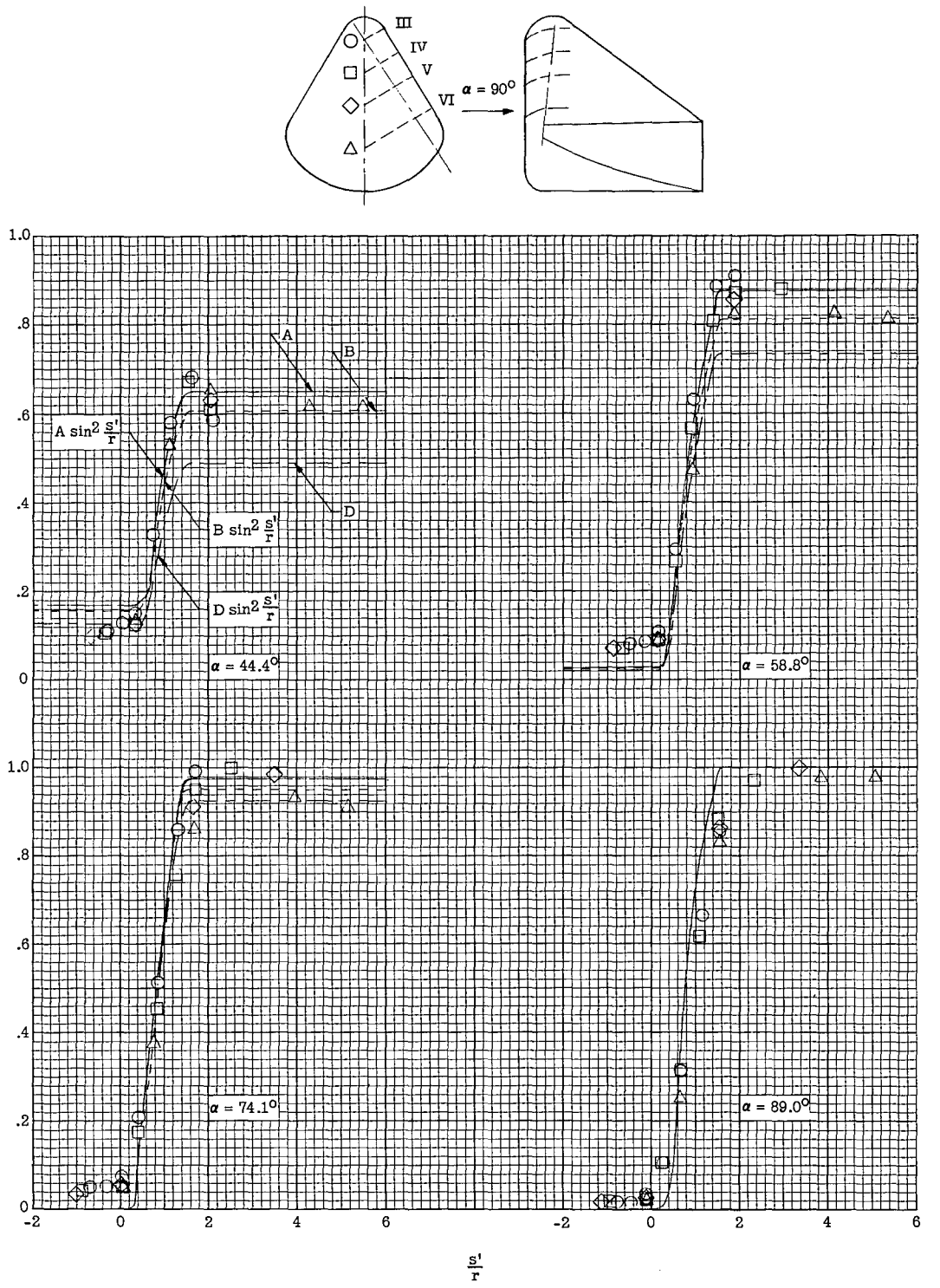

Figure 11.- Comparison of measured pressure data on leading edge of delta planform with data obtained by use of an expression related to sweep and impact theory.

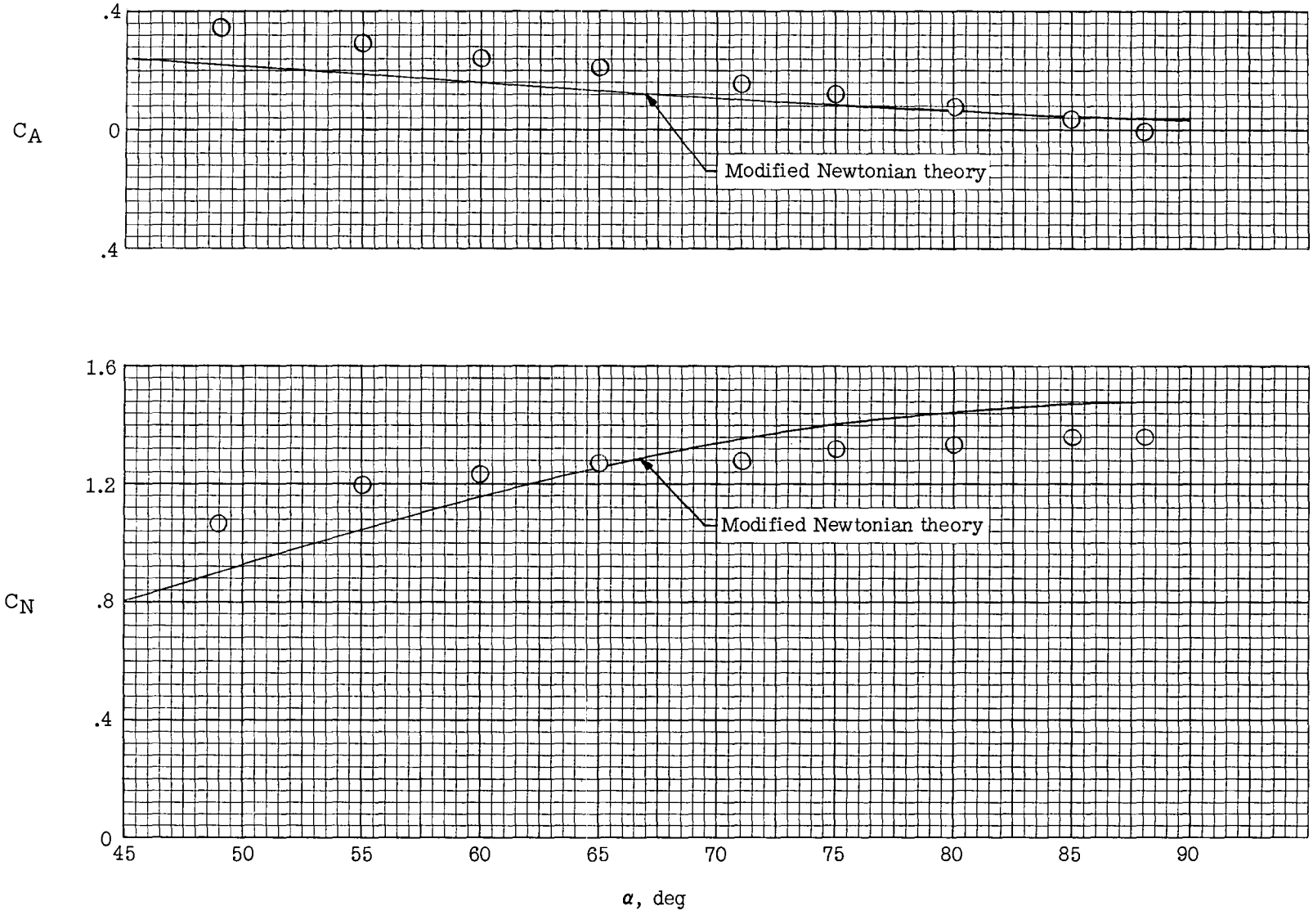

Figure 12.- Comparison of measured force data from reference 7 with integrated modified Newtonian predictions.